ОБЪЕДИНЕННЫЙ
ИНСТИТУТ
ЯДЕРНЫХ
ИССЛЕДОВАНИЙ

Дубна

E2-96-119

D.Ebert*[1], M.K.Volkov*

KAON POLARIZABILITY IN THE NAMBU—JONA-LASINIO MODEL AT ZERO AND FINITE TEMPERATURE

Submitted to «Ядерная физика»

*Supported by Deutsche Forschungsgemeinschaft under contract 436 RUS 113/29

[1]On leave of absence of Institut für Physik, Humboldt-Universität zu Berlin, Invalidenstrasse 110, D-10115 Berlin, Germany

1996

1. Introduction

There is a renewed interest in electromagnetic polarizabilities of the pion and kaon which together with other low-energy parameters like electromagnetic radii provide us with useful information on the internal structure of mesons (for a review on recent results obtained in different models see e.g. refs. [1, 2, 3]). Some of us calculated these polarizabilities earlier within nonlinear chiral hadron theories [4, 5] as well as on the basis of a bosonized NJL-model [6] leading to a linear σ-model [7, 8]. In the linear σ-model pole diagrams arising from intermediate scalar mesons[1] ϵ, $f_0(980)$ and $a_0(980)$ turn out to play an important role in the calculation of meson polarizabilities. In particular, for describing the physical isoscalar scalar mesons ϵ and f_0 within an underlying quark model, one has to take into account the mixing angle θ of the (u,d) and (s) quark content of these mesons (see [7]).

In the latter paper strong and radiative decays of scalar mesons were investigated solely on the level of quark loop triangle diagrams. In the papers [11, 12] it was however argued that additional meson loop contributions can play an important role for the description of the scalar meson decays.[2] This idea does not contradict the usual $1/N_c$ expansion since both quark and meson loops turn out to be of the same order in N_c for this case. Stimulated by these arguments we have recalculated the decay amplitudes of scalar mesons. We found that pion and espacially kaon loops turned out to be indeed essential for the description of the decay $f_0 \to \gamma\gamma$, which is crucial for the determination of the mixing angle on the basis of new experimental data. We find a value $\theta = 23°$ for the mixing angle, which would change to $\theta = -18°$ if meson loops were omitted.

Clearly, changes of the mixing angle also significantly influence other physical quantities, like the kaon polarizability. Therefore, we apply the new results to estimate the kaon polarizability.

In the last part of our paper, we have investigated the temperature dependence of the kaon polarizabilities. The behaviour of hadrons at finite T, espacially near the critical point where the chiral symmetry restoration takes place, is a very interesting problem. This problem is now actual because it is planned to put into operation the new particle accelarators (RHIC at Brookhaven, LHC at CERN, etc), where heavy-ion collisions will be investigated.

This paper is organized as follows. In Section 2, we give the Lagrangians and calculate the mixing angle. In Section 3, we calculate the kaon polarizability using the new value for the mixing angle. The temperature dependence of the kaon polarizability is considered in Section 4. We summarize and conclude in Section 5.

2. Lagrangians and determination of the mixing angle

For definiteness, let us consider meson vertices generated by quark loops arising in the bosonization approach of QCD-motivated quark-models [7, 6]. Then, the corresponding local terms satisfy approximate chiral symmetry of the resulting effective meson lagrangian in the case of $m_s \neq m_u$, where m_s and m_u are the constituent masses of strange or (u,d)-quarks, respectively. First, let us quote only that part of the meson lagrangian which describes the decays of scalar mesons $\epsilon(650)$, $f_0(980)$ and $a_0(980)$ into two pions and kaons [8] (see Fig. 1a)

$$\begin{aligned}\mathcal{L}_1 &= \sum_{S=\epsilon,f_0} \left(G_\pi^S\, \vec{\pi}^2(x)\, S(x) + G_K^S\, \bar{K}(x)\, K(x)\, S(x)\right) \\ &\quad + G_K^{a_0}\, \bar{K}(x)\, \tau_3\, K(x)\, a_0(x)\ , \end{aligned} \tag{1}$$

where

$$\begin{aligned} G_\pi^\epsilon &= 2\, g_\pi\, Z^{1/2}\, m\, \cos\theta\ , \\ G_\pi^{f_0} &= 2\, g_\pi\, Z^{1/2}\, m\, \sin\theta\ , \\ G_K^\epsilon &= 2\, g_K\, Z^{1/2}\, \left[(2m - m_s)\, \cos\theta + \sqrt{2}\,(2m_s - m)\, \sin\theta\right]\ , \end{aligned}$$

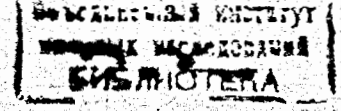

[1] The ϵ meson is considered to be a broad resonance with mass and width which are not presently completely fixed yet [9]. We shall use here the theoretical value of the mass $M_\epsilon^{theor} = 650$ MeV and the new experimental value $M_\epsilon^{exp} = 750$ MeV [9]. The masses of the other scalar mesons are given by $M_{f_0} = 980$ MeV and $M_{a_0} = 982$ MeV [10].

[2] Note that in the case of $a_0 \to \gamma\gamma$ the additional effect of meson loops only weakly changes the result in contrast with the result of ref. [12] where the effect of 50% was found, and quark and meson loops interfere in a destructive way, while we found both effects to be additive. In [11] only scalar meson loops were considered.

$$G_K^{f_0} = 2\,g_K\,Z^{1/2}\left[(2m-m_s)\sin\theta-\sqrt{2}\,(2m_s-m)\cos\theta\right],$$
$$G_K^{a_0} = 2\,g_K\,Z^{1/2}\,(2m-m_s)\,. \qquad (2)$$

Besides the Goldberger-Treiman relations $g_\pi = m/F_\pi$, $g_K = (m_u+m_s)/(2F_K)$, we shall use the following parameter values $F_\pi = 93$ MeV, $F_K = 1.16\,F_\pi$, $m_u = m_d = m = 280$ MeV, $m_s = 450$ MeV. Here Z is a renormalization coefficient arising from π-A_1-mixing ($Z \approx 1.4$ [7]).

Below we shall determine the mixing angle θ, which describes the deviation of the singlet-octet mixing angle from the ideal mixing by using recent experimental data for $f_0 \to 2\gamma$ and $f_0 \to 2\pi$. For this, we remind that the scalar components of the ideal mixing are related to the physical meson states through

$$(\sigma_8+\sqrt{2}\,\sigma_0)/\sqrt{3} = \epsilon\cos\theta + f_0\sin\theta\,,$$
$$(\sqrt{2}\,\sigma_8-\sigma_0)/\sqrt{3} = f_0\cos\theta-\epsilon\sin\theta\,. \qquad (3)$$

Now, let us consider two-photon decays of scalar mesons which are described by finite quark and meson loop diagrams (see Fig. 1 b - d).

The amplitude of the decay $S \to 2\gamma$ arising from quark loops takes the form

$$T^{q\mu\nu} = (g^{\mu\nu}\,q_1q_2 - q_2^\mu\,q_1^\nu)\,T^q\,, \qquad (4)$$

where

$$T^q = \frac{2}{9}\,\frac{\alpha\;a_S}{\pi F_\pi Z^{1/2}}\,. \qquad (5)$$

Here $q_{1,2}$ are the photon momenta, $\alpha = 1/137$ and the coefficient a_S is given by

$$a_\epsilon = 5\cos\theta + \sqrt{2}\,\frac{F_\pi}{F_S}\sin\theta\,,$$
$$a_{f_0} = 5\sin\theta - \sqrt{2}\,\frac{F_\pi}{F_S}\cos\theta\,,$$
$$a_{a_0} = 3\,, \qquad (6)$$

with $F_S = 1.28\,F_\pi$ [7]. Here we have used low-momentum expansion around $q_1\cdot q_2 \approx 0$. In refs., [6, 7, 13] it has been shown that this prescription respects $SU(3)_F$-symmetry and leads to reasonable results for 2 photon decays of the pseudoscalar meson nonet.

Let us next calculate the meson loop contributions of Figs. 1c,d which, due to $G^S \sim g_S \sim 1/\sqrt{N_c}$, contribute in the same order of the $1/N_c$ expansion as the quark loop diagrams. Taking into account the Lagrangian of electromagnetic interactions

$$\mathcal{L}_2 = i\,e\,A^\mu\,(\pi^-\,\partial_\mu\pi^+ - \pi^+\,\partial_\mu\pi^- + K^-\,\partial_\mu K^+ - K^+\,\partial_\mu K^-)$$
$$+e^2\,A_\mu^2\,(\pi^+\pi^- + K^+K^-)\,, \qquad (7)$$

one easily obtains

$$T^{m\mu\nu} = (g^{\mu\nu}\,q_1q_2 - q_2^\mu q_1^\nu)\,T^m\,, \qquad (8)$$

with

$$T^m = G_M^S\,\eta\,\frac{\alpha}{2\pi}\,\frac{2}{M_S^2}\,[x_M\,\phi(x_M)-1]\,, \qquad (9)$$

where the function $\phi(x)$ is defined by

$$\phi(x) = \begin{cases} \left[\arctan(x-1)^{-1/2}\right]^2\,, & x \geq 1 \\ \left[\frac{i}{2}\ln\frac{1-\sqrt{1-x}}{1+\sqrt{1-x}} - \frac{\pi}{2}\right]^2\,, & x \leq 1\,. \end{cases} \qquad (10)$$

and $x_M = \frac{2M^2}{q_1q_2} = \left(\frac{2M}{M_S}\right)^2$, $\eta = 2(1)$ for pions (kaons), and M is the mass of the meson circulating in the loop.

Then we use these results for the determination of the mixing angle θ from the decays $f_0 \to \gamma\gamma$ and $f_0 \to \pi\pi$. Taking into account expressions (5) and (9), the total amplitude for the decay $f_0 \to 2\gamma$ consisting of quark, pion and kaon loops, reads[3]

$$T_{f_0\to\gamma\gamma} = T^q_{f_0\to\gamma\gamma} + T^\pi_{f_0\to\gamma\gamma} + T^K_{f_0\to\gamma\gamma}\,,$$
$$T^q_{f_0\to\gamma\gamma} = \frac{\alpha}{\pi F_\pi}\,(-0.2\cos\theta + 0.9\sin\theta)\,,$$
$$T^\pi_{f_0\to\gamma\gamma} = \frac{\alpha}{\pi F_\pi}\,(-0.4+0.19\,i)\sin\theta\,,$$
$$T^K_{f_0\to\gamma\gamma} = \frac{\alpha}{\pi F_\pi}\,(-0.7\cos\theta + 0.1\sin\theta)\,,$$
$$T_{f_0\to\gamma\gamma} = -0.9\,\frac{\alpha}{\pi F_\pi}\sin\theta\,(\cot\theta - 0.7 - 0.21\,i)\,. \qquad (11)$$

[3]Small contributions of loop diagrams with non-strange scalar mesons (10% of $T^\pi_{f_0\to\gamma\gamma}$) and strange scalar mesons (4% of $T^K_{f_0\to\gamma\gamma}$) will be omitted.

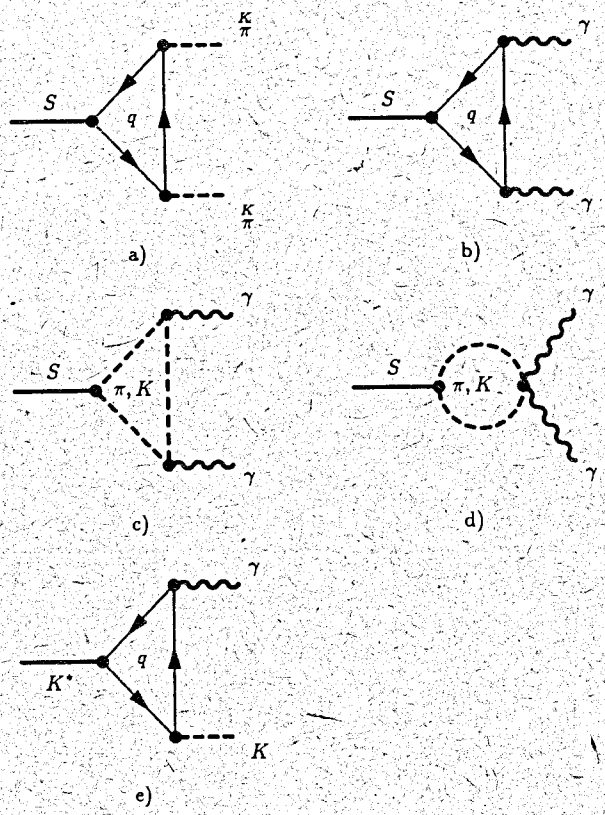

Fig.1 The triangle quark-loop diagrams, describing the decays:
a) $S \to 2\pi$ $(2K)$, b) $S \to 2\gamma$, e) $K^* \to \gamma K$.
c) The triangle meson-loop diagrams, describing the decays $S \to 2\gamma$.
d) The meson-loop diagrams, describing the decays $S \to 2\gamma$.

Now, using the Lagrangian $\mathcal{L}_1$ and the amplitude (11), we obtain the following expressions for the decay widths of $f_0 \to \gamma\gamma$ and $f_0 \to \pi\pi$

$$\Gamma_{f_0\to\gamma\gamma} = \frac{M_{f_0}^3}{64\pi} \left|T_{f_0\to\gamma\gamma}\right|^2 , \tag{12}$$

$$\Gamma_{f_0\to\pi\pi} = \frac{3Z}{2\pi M_{f_0}} \left(\frac{m^2}{F_\pi}\right)^2 \sqrt{1-\left(\frac{2M_\pi}{M_{f_0}}\right)^2}\, \sin^2\theta . \tag{13}$$

By comparing their ratio with the experimental value [10]

$$\frac{\Gamma_{f_0\to\gamma\gamma}}{\Gamma_{f_0\to\pi\pi}} = 1.5\cdot 10^{-5} , \tag{14}$$

we obtain two solutions, $\theta = 23°$ and $\theta = -43°$. The choice $\theta = 23°$ leads to predictions

$$\Gamma_{f_0\to\gamma\gamma} = 1.1 \text{ keV} ,$$
$$\Gamma_{f_0\to\pi\pi} = 72 \text{ MeV} ,$$

which are somewhat larger than the averaged values of PDG [10]. It is worth mentioning that discarding meson loops would even yield a negative angle $\theta \sim -18°$.

For later applications, let us also quote the effective Lagrangian describing the radiative decay $K^* \to K\gamma$ of vector mesons corresponding to the anomalous quark triangle diagram shown in Fig. 1e,

$$\mathcal{L}_3 = \frac{e\, g_V}{32\,\pi^2\, F_K}\, a_{K^*}\, \epsilon^{\sigma\kappa\nu\mu}\, F_{\kappa\nu}(x)\, K^*_{\sigma_\mu}(x)\, K(x) , \tag{15}$$

with $g_V = g_\rho$ being the vector meson coupling constant $(g_\rho^2/(4\pi) \approx 3)$. Moreover, using the value of the quark mass ratio $\lambda = m_u/m_s \sim 0.62$, the coefficients a_{K^*} are estimated as [8]

$$a_{K^{*+}} = \frac{1}{2}\left[1 - \frac{2\lambda}{1-\lambda^2}\left(3 + \frac{2+\lambda^2}{1-\lambda^2}\ln\lambda^2\right)\right] \simeq 1.2 ,$$
$$a_{K^{*0}} = 1 - \frac{\lambda}{1-\lambda^2}\ln\lambda^2 \simeq 2 . \tag{16}$$

Finally, we need the box-diagram describing the low-energy Compton effect off K mesons, shown in Fig. 2. This diagram leads to the Lagrangian term

$$\mathcal{L}_4 = \frac{\alpha}{18\pi\, F_K^2}\, F_{\mu\nu}^2(x)\left(K^+(x)\,K^-(x) + 4\,K^0(x)\bar{K}^0(x)\right) . \tag{17}$$

3. Kaon polarizability

In nonlinear chiral models [5] (arising in the limit $M_S \to \infty$) and in the chiral-symmetry limit of the linear σ-model [8] the main contributions to the polarizability of charged kaons and pions emerge from pole diagrams with intermediate scalar mesons containing the quark loop vertices shown in Fig. 1a,b [4]. This is contrary to the case of neutral mesons where the contributions of the corresponding pole diagrams are completely cancelled by the box diagrams shown in Fig. 2.

Beyond the chiral limit, this situation still holds for pions, whereas for kaons the result strongly depends on the value of the mixing angle. We will find below that for $\theta = 23°$ the scalar meson contribution is reduced by about 50% with respect to the value of the chiral limit but still dominates the box diagram contribution. For neutral kaons the contribution of pole diagrams remains somewhat dominant with respect to the box diagram term, leading to a small nonvanishing value of the neutral kaon polarizability. To see this in more detail, let us write the contributions of scalar meson pole and box diagrams to the kaon polarizability $\alpha_K^{(S+b)}$ in the form[5]

$$\begin{aligned} \alpha_{K^+}^{(S+box)} &= C\,(2\,\Delta_+ - 1)\,, \\ \alpha_{K^0}^{(S+box)} &= C\,(2\,\Delta_- - 4)\,, \qquad C = \frac{\alpha}{18\pi\, F_K^2\, M_K}\,, \end{aligned} \tag{18}$$

where

$$\begin{aligned} \Delta_\pm \;=\; & (m_s + m)\left\{ \frac{a_\epsilon}{M_\epsilon^2}\left[(2m - m_s)\cos\theta + \sqrt{2}(2m_s - m)\sin\theta\right]\right. \\ & - \frac{a_{f_0}}{M_{f_0}^2}\left[\sqrt{2}(2m_s - m)\cos\theta - (2m - m_s)\sin\theta\right] \\ & \left. \pm \frac{a_{a_0}}{M_{a_0}^2}(2m - m_s)\right\}\,. \end{aligned} \tag{19}$$

[4] The contribution of meson loop diagrams will be discussed later on (see Fig. 3).

[5] Recall that the electric and magnetic polarizabilities α_P, β_P of pseudoscalar mesons are obtained from the low-energy Compton amplitude by the decomposition

$$T_{NR} \;=\; -\vec{\epsilon}\cdot\vec{\epsilon}\,'\,\frac{\alpha}{M} + \vec{\epsilon}\cdot\vec{\epsilon}\,'\,\omega\omega'\,\alpha_P + (\vec{\epsilon}\times\vec{k})\cdot(\vec{\epsilon}\,'\times\vec{k}')\,\beta_P\,,$$

with $\omega\,(\omega')$, $k\,(k')$ and $\epsilon\,(\epsilon')$ being the incoming (outgoing) photon energy, momentum and polarization, respectively.

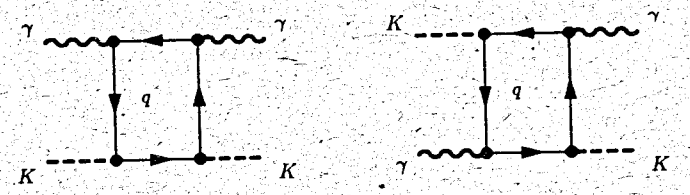

Fig.2 The quark-box diagrams, describing the Compton effect off kaons.

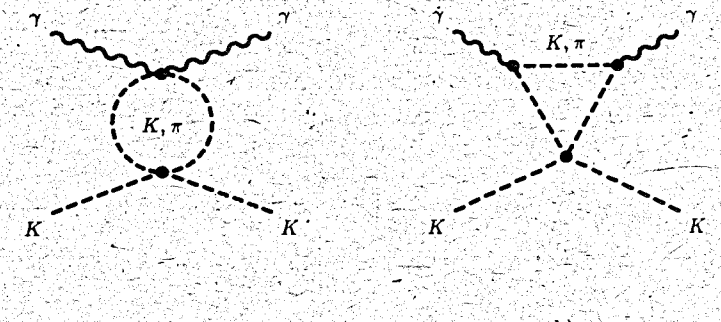

Fig.3 The meson-loop diagrams, describing the Compton effect off kaons.

Taking into account (6), $\theta = 23^\circ$ and using two different values of the ϵ-mass, $M_\epsilon = 650$ (750) MeV, we obtain $\Delta_+ = 3.55$ (2.6), $\Delta_- = 3.05$ (2.1). This leads to the following estimates

$$\begin{aligned} \alpha_{K^+}^{(S+box)} &\simeq C\,(7.7(5.8) - 1.1 + 0.5 - 1) = 10.5(7.2)\cdot 10^{-4}\,\mathrm{fm}^3\,, \\ \alpha_{K^0}^{(S+box)} &\simeq C\,(7.7(5.8) - 1.1 - 0.5 - 4) = 3.65(0.34)\cdot 10^{-4}\,\mathrm{fm}^3\,. \end{aligned} \tag{20}$$

For illustration, let us compare (20) with the results obtained in the chiral symmetry limit ($\theta = 0$, $M_\epsilon^2 = M_{f_0}^2 = M_{a_0}^2 \simeq 4m^2$). In this case we have

$$\begin{aligned} \alpha_{K^+}^{(S+box)} &\simeq C\,(5 + 2 + 3 - 1) = 15.4\cdot 10^{-4}\,\mathrm{fm}^3\,, \\ \alpha_{K^0}^{(S+box)} &\simeq C\,(5 + 2 - 3 - 4) = 0\,, \end{aligned} \tag{21}$$

where the first three terms in the brackets of (20) and (21) denote the pole contributions of ϵ, f_0 and a_0 mesons whereas the last terms denote the contribution of the box diagrams. Thus, the deviation from chiral symmetry in combination with the above mixing angle influences the polarizability. For $\theta = 23^\circ$ the contribution of the f_0-meson has not only decreased in absolute value but even changed in sign compared to the chiral limit, whereas the a_0-contribution is reduced by an order of magnitude.

Scalar meson pole diagrams and box diagrams supply also analogous contributions to the magnetic polarizability $\beta_K^{(S+box)}$ but with the opposite sign ($\alpha_K^{(S+box)} = -\beta_K^{(S+box)}$).

In addition, a large contribution to the magnetic polarizability of neutral kaons arises from pole diagrams containing the intermediate vector meson K^*. It can easily be evaluated using the Lagrangian $\mathcal{L}_3$ which leads to the result

$$\beta_K^{(K^*)} = -\left(\frac{a_{K^*}}{2\pi F_K}\right)^2 \frac{\alpha\,\alpha_V\,M_K}{M_{K^*}^2 - M_K^2} = \begin{cases} 4.9\cdot 10^{-4}\,\mathrm{fm}^3 & (K^+) \\ 12.7\cdot 10^{-4}\,\mathrm{fm}^3 & (K^0)\,. \end{cases} \tag{22}$$

For completeness, let us consider the meson loop diagrams shown in Fig. 3, leading to additional contributions to the kaon polarizability comparable to the values obtained from (18). These contributions have first been evaluated in ref. [4] for a nonlinear chiral theory, providing a suitable low-energy approximation of the linear σ-model. The

expression of the Compton-amplitude associated with the diagrams exhibited in Fig. 3, reads

$$\begin{aligned} T_\pm^{\mu\nu} &= \frac{2\alpha}{4\pi F_K^2}\,(g^{\mu\nu}\,q_1\cdot q_2 - q_1^\nu\,q_2^\mu)\left[\beta^{(\pi)}(q_1q_2) + \beta_\pm^{(K)}(q_1q_2)\right]\,, \\ T_0^{\mu\nu} &= \frac{2\alpha}{4\pi F_K^2}\,(g^{\mu\nu}\,q_1\cdot q_2 - q_1^\nu\,q_2^\mu)\left[\beta^{(\pi)}(q_1q_2) + \beta_0^{(K)}(q_1q_2)\right]\,. \end{aligned} \tag{23}$$

The function $\beta^{(\pi)}(q_1q_2)$ arising from the above two loop diagrams with internal pion lines is equal for charged and neutral kaons,

$$\beta^{(\pi)}(q_1q_2) = \frac{1}{2}\left[\tilde{x}_\pi\,\phi(\tilde{x}_\pi) - 1\right] \overset{q_1q_2\to 0}{\longrightarrow} 0\,. \tag{24}$$

The function $\beta_\pm^{(K)}$ describes the contribution of the loop diagrams of Fig. 3 with internal kaon propagators and external charged kaons,

$$\beta_\pm^{(K)} = \frac{1}{4}\,(\tilde{x}_K + 1)\,\left[\tilde{x}_K\,\phi(\tilde{x}_K) - 1\right] \overset{q_1q_2\to 0}{\longrightarrow} \frac{1}{12}\,. \tag{25}$$

For external neutral kaons we get

$$\beta_0^{(K)} = \left[\tilde{x}_K\,\phi(\tilde{x}_K) - 1\right] \overset{q_1q_2\to 0}{\longrightarrow} 0\,. \tag{26}$$

Thus, for $(q_1\cdot q_2) = 0$ a nonvanishing contribution to the kaon polarizability arises only from $\beta_\pm^{(K)}(0) = 1/12$ leading to the result

$$\alpha_{K^\pm}^{(K)} = \frac{\alpha}{4\pi F_K^2\,M_K}\,\beta_\pm^{(K)}(0) \simeq 0.6\cdot 10^{-4}\ \mathrm{fm}^3 = -\beta_{K^\pm}^{(K)}\,. \tag{27}$$

For neutral kaons the meson loop contribution to the polarizability vanishes.

We shall not calculate here the contributions of intermediate axial vector mesons (A) to the polarizability. The corresponding pole diagrams have been investigated in [7, 8],

$$\alpha_{K^\pm}^{(A)} = 0.9\cdot 10^{-4}\ \mathrm{fm}^3\,, \qquad \alpha_{K^0}^{(A)} = 0.5\cdot 10^{-4}\ \mathrm{fm}^3\,. \tag{28}$$

We mention that a noticeable contribution, compared to the other terms, was obtained only for the electric polarizability of charged kaons. Table 1 summarizes our estimates for the electric (α_K) and magnetic (β_K) polarizabilities as obtained from quark box diagrams

	box	S	M	V	A	Total	chiral limit
α_{K^+}	- 1.7	12.2 (8.9)	0.6	0	0.9	12 (8.7)	16.9
α_{K^0}	- 6.8	10.5 (7.2)	0	0	0.5	4.2 (0.9)	0.5
β_{K^+}	1.7	-12.2 (-8.9)	-0.6	4.9	0	-6.2 (-2.9)	-11.1
β_{K^0}	6.8	-10.5 (-7.2)	0	12.7	0	9.0 (12.3)	12.7

Table 1: Electric and magnetic polarizabilities of kaons in units of 10^{-4} fm^3. The columns show the contributions from quark box diagrams (box), scalar meson poles (S), meson loops (M) and intermediate vector (V) and axial vector (A) mesons. The pole contributions are estimated for two values of the ϵ-mass, $M_\epsilon =$ 650(750) MeV.

(box), scalar meson pole diagrams (S), meson loop diagrams (M), intermediate vector (V) and axial vector (A) mesons. Thus, in comparision with the results of the chiral symmetry limit, for the realistic case of physical scalar meson masses and the mixing angle $\theta = 23°$ a slightly increased value of the electric polarizability should be observed for neutral kaons, whereas the electric and magnetic polarizabilities for charged kaons are reduced. For future comparision with data let us also quote the sum of the electric and magnetic kaon polarizabilities

$$\begin{aligned} (\alpha+\beta)_{K^+} &= 5.8 \cdot 10^{-4}\ \text{fm}^3\ , \\ (\alpha+\beta)_{K^0} &= 13 \cdot 10^{-4}\ \text{fm}^3\ . \end{aligned} \tag{29}$$

Note that our results satisfy the requirement $(\alpha+\beta)_K > 0$ from dispersion relations [1].

4. Temperature dependence of the kaon polarizabilities

In the previous sections we have shown that the mixing angle θ plays a very important role for the definition of the main contributions to the kaon polarizabilities associated with the scalar pole diagrams (see, also, [14]). Unfortunately, within our model, one cannot define the temperature dependence of the mixing angle. Let us suppose that

θ has to decrease with T and to equal zero when $T = T_c$ (T_c is the critical T). Since the quark condensate is the order parameter in the NJL model, also decreasing with T, we assume that θ is proportional to the quark condensate or, equivalently, to the constituent quark mass m: $\theta(T) = \theta\ \frac{m(T)}{m(0)}$. Clearly, this is a very crude approximation, so that we can obtain here only qualitative estimations of the T-dependence of the kaon polarizabilities.

In order to obtain the T-dependence of the other physical parameters $m, m_s, M_\pi, M_K, F_\pi$ and F_K we can use the results of our earlier works [15]. The correspondiong values are given in Table II.

T	m_u	m_s	M_π	M_K	F_π	F_K
0	280	450	137	494	93	108
50	280	450	137	494.5	93	107
100	271	448.5	137	502	91	104.6
150	223	437	138	519	82	97
170	184	427	141	531	73	91
180	158	420.6	146	541	65	87
190	127	413.5	155	555	55	82
200	95	405	172	574	43	76

Table II. The temperature dependence of the constituent quark masses m and m_s, the pion and kaon masses and their decay coupling constants F_π and F_K. All values are given in MeV.

For the scalar meson masses M_ϵ, M_{f_0} and M_{a_0} we shall use the approximate mass formulae $M^2_\epsilon(T) = const + 4m^2(T)$, $M^2_{f_0}(T) = const' + 4m^2_s(T)$, $M^2_{a_0}(T) = const'' + 4m^2(T)$, and $M_{K^*}(T) \approx M_{K^*}(0)$. [6] For the definition of the temperature dependence of the axial-vector meson contributions we shall use a formula similar to (22) (see [7, 8])

$$\alpha_K^{(A)} = C\ \frac{M_K}{F_K^2 (M^2_{K_1(1270)} - M^2_K)}, \tag{30}$$

[6] As is shown in [15] the temperature dependence of the scalar mesons is defined by their quark mass terms (for instance, $M^2_\epsilon(T) \approx M^2_\pi(T) + 4m^2(T)$, where $m(T)$ varies more rapidly wit T than $M_\pi(T)$). The vector meson masses are stable with respect to temperature change.

where $C = 3.8\ 10^{-4}$ and $M^2_{K_1(1270)}(T) \approx 0.857\ GeV^2 + 6m(T)m_s(T)$ $(M_{K_1} = 1270MeV)$. [7]

T	0	50	100	150	170	180	190	200
$\alpha^S_{K^+}=-\beta^S_{K^+}$	12.2	12.6 (12.6)	12.8 (12.8)	12.2 (14)	9.8 (14.8)	6.7 (15)	0.54 (14.6)	-9.4 (13.5)
$\alpha^S_{K^0}=-\beta^S_{K^0}$	10.5	11.1 (11.2)	11.4 (11.6)	12 (14)	11 (16)	8.4 (16.8)	3.4 (17.6)	-5.4 (16.5)
$\alpha^{box}_{K^+}=-\beta^{box}_{K^+}$	-1.7	-1.7	-1.8	-2	-2.2	-2.4	-2.6	-3
$\alpha^{box}_{K^0}=-\beta^{box}_{K^0}$	-6.8	-7	-7.2	-8.1	-9	-9.6	-10.6	-11.9
$\beta^V_{K^+}$	4.9	5	5.3	7.2	9.0	10.6	12.8	15.8
$\beta^V_{K^0}$	12.7	13	13.6	16.4	18.7	20.5	23	26
$\alpha^A_{K^+}$	0.9	0.9	1	1.4	1.8	2.2	2.3	3.8
$\alpha^A_{K^0}$	0.5	0.5	0.6	0.8	1	1.2	1.3	2.1
$\alpha^{tot}_{K^+}$	11.4	11.8	12	11.6	9.4	6.5	0.2	-8.6
$\alpha^{tot}_{K^0}$	4.2	5	4.8	4.7	2.9	0	-5.9	-15
$\beta^{tot}_{K^+}$	-5.6	-5.9	-5.7	-3	1.4	6.3	15	28
$\beta^{tot}_{K^0}$	9	8.9	9.4	12.5	16.8	21.7	30	43

Table III contains the temperature depending contributions to the electric and magnetic kaon polarizabilities of the scalar pole diagrams, box, vector meson pole and axial meson pole diagrams. In the brackets we give the results corresponding to the case when $\theta(T) = const$. The units are $10^{-4}\ fm^3$ for the polarizabilities. Here, we have ignored the meson loop contributions.

Let us discuss the temperature dependence of different contributions to the kaon polarizabilities. As Table III shows, the scalar pole contributions remain approximately constant up to $T \approx 170MeV$ and then monotonously decrease changing the sign at $190MeV$ (charge kaon) and $180MeV$ (neutral kaon). On the other hand, the contributions of the box diagrams, the vector and axial vector pole diagrams monotonically increase in their absolute values. In summary, the total electric kaon polarizabilities are approximately stable in the temperature interval $0 < T < 150MeV$ and then monotonically decrease, changing their signs for $T > 180MeV$ (charge kaon) and $T > 170MeV$ (neutral kaon). The magnetic kaon polarizabilities monotonically increase in the whole temperature domain. In particular, the charged magnetic polarizability changes the sign for $T > 150MeV$. Note that for a constant mixing angle (see values in brackets) the scalar meson pole contributions would weakly increase until $T \approx 190MeV$.

[7] Here we shall ignore the weak temperature dependence of the quark loop diagrams with the photon legs. The temperature dependence of these diagrams is especially weak when the relatively heavy strange quark is contained in the quark loop. The temperature dependence of these diagrams has been investigated in [17].

5. Summary and Conclusions

In this paper, we have estimated the mixing angle of scalar mesons within a chiral quark σ-model from the decays $f_0 \to \gamma\gamma$, $f_0 \to \pi\pi$ using new data [10] and taking into account both quark and meson loop diagrams. The new value of the mixing angle $\theta = 23°$ obtained by including meson loops, significantly differs from the value $\theta = -18°$ which would have been obtained if only quark loops were taken into account. The value $\theta = 23°$ is then used to estimate the polarizability of kaons. For this aim, we have calculated the low-energy Compton amplitude for K mesons, taking into account scalar pole diagrams as well as box and triangle diagrams including quark and meson loops. As Table 1 shows, scalar meson poles give an important contribution to the electric and magnetic polarizabilities of charged and neutral mesons. The dominant scalar meson contributions arise here from ϵ and f_0, whereas the contribution of a_0 is relatively small.

Notice that our model allows one to study the deviation from the chiral symmetry limit ($M_\epsilon = M_{f_0} = M_{a_0} = 2m$; $\theta = 0$). As we have found, for the realistic case of physical scalar meson masses and a mixing angle $\theta = 23°$ the absolute values of the electric and magnetic polarizabilities for charged kaons are reduced by about 50%, whereas the electric polarizability of neutral kaons increases. In the latter case, the results turn out to be rather sensitive to changes of the ϵ-mass.

It is interesting to compare our results with predictions of other

models. For example, the results of the Quark Confinement Model (QCM) [16] for the charged pion polarizability are close to the predictions of our model in ref. [8, 17], whereas they are larger by a factor 2–4 in the case of the kaon polarizability. An analogous result as in [16] was obtained for neutral kaons in an $SU(3)$ NJL-model [18].

In conclusion, let us emphasize that we have obtained our results in the framework of the standard NJL model. In this model one considers only the first terms of the momentum expansion of the quark loop diagrams without taking into account their dependence on the momentum of the external meson legs. However, it is worth noticing that taking into account such a momentum dependence for box and triangle quark diagrams could lead to an additional momentum-dependent factor $f(p_K^2)$ (see [17])

$$f(p_K^2) = 6(m+m_s)\int_0^\infty dk k^2 \frac{E_u+E_s}{E_u E_s[(E_u+E_s)^2-p_K^2]^2}, \quad (31)$$

where $E_i=\sqrt{m_i^2+k^2}$ and p_K is the kaon momentum.

Then, our formulae (18) and (22) take the form

$$\alpha_{K^+}^{S+box} = C\,(2\,\Delta_+ - f(M_K^2)) \quad (32)$$

$$\alpha_{K^0}^{S+box} = C\,(2\,\Delta_- - 4\,f(M_K^2)) \quad (33)$$

and

$$\alpha_K^{K^*} = (\frac{a_{K^*}}{2\pi F_K})^2 \frac{\alpha\alpha_V M_K}{M_{K^*}^2-M_K^2}\,(f(M_K^2))^2 \quad (34)$$

Neglecting the p_K^2 dependence in $f(p_K^2)$ reproduces our former results (18) and (22) because $f(0)\approx 1$. However, the function $f(M_K^2)$ has a nontrivial dependence on the temperature. Indeed, the function $f(M_K^2)$ has a singular behaviour near the so-called Mott-temperature, when $T>T_{Mott}$, where $M_K(T)>m_u(T)+m_s(T)$. (The Mott temperature is the temperature, when the kaon mass becomes equal to the sum of masses of its quark components: $M_K(T_{Mott})=m_u(T_{Mott})+m_s(T_{Mott})$. In our model $T_{Mott}\approx 187MeV$.) Then, the contributions to the kaon polarizabilities of the corresponding diagrams could very

T	0	50	100	150	170	180	185	190
$f(M_K^2)$	1.6	1.62	1.65	2.03	2.74	4.21	8.3	∞

Table IV. Values of the function $f(M_K^2)$ at different T.

strongly increase near the Mott-point (see Table IV, where values of the function $f(M_K^2)$ are given at different values of T).

The physical meaning of this effect is transparent. Before the transition into the quark-gluon plasma the dipole momentum of the meson strongly increases, and then we observe the dissociation of the meson into their quark components.

Clearly, a more quantitative discussion of the temperature behaviour of the kaon polarizabilities near the Mott point is beyond the scope of the local NJL model. It would be interesting to investigate this effect more carefully in realistic nonlocal quark models including confinement and meson form factors.

One of the authors (M.K.V.) would like to thank Prof. J. Hüfner for the useful discussions. This work was partially supported by the European Community via INTAS (94-2915).

References

[1] J. Portoles and M.R. Pennington, Preprint University of Durham, DTP-94/52 (1994).

[2] S. Bellucci, *Proceedings of Chiral Dynamics* Workshop at MIT (1994), ed. by A.M. Bernstein and B.R. Holstein, Springer Berlin, Heidelberg (1995).

[3] J. Gasser, *Proceedings of Chiral Dynamics* Workshop at MIT (1994), ed. by A.M. Bernstein and B.R. Holstein, Springer Berlin, Heidelberg (1995).

[4] M.K. Volkov and V.N. Pervushin, Sov. J. Nucl. Phys. **22** (1975) 179; Phys. Lett. **B55** (1975) 405; ibid. **B58** (1975) 177; Nuovo Cim. **27** (1975) 277.

[5] D. Ebert and M.K. Volkov, Phys. Lett. **B101** (1981) 252.

[6] D. Ebert and M.K. Volkov, Sov. J. Nucl. Phys. **36** (1982) 736; Z. Phys. **C16** (1983) 205.
M.K.Volkov, Ann. Phys. **157** (1984) 282.
D. Ebert and H. Reinhardt, Nucl. Phys. **B271** (1986) 188.

[7] M.K. Volkov, Sov. J. Part. and Nucl. **17** (1986) 186.

[8] M.K. Volkov, and A.A. Osipov, Sov. J. Nucl. Phys. **41** (1985) 659.

[9] G.Z. Mennessier, Z. Phys. **C16** (1983) 241;
M. Svec, A. de Lesquen and L. van Rossum, Phys. Rev. **D46** (1992) 949;
M. Svec, hep-th/9511205 (1995).

[10] Review of Part. Properties, Phys. Rev. **D50** (1994), 1173.

[11] A.I. Vainshtein, M.B. Voloshin, V.A. Zakharov and M.A. Shifman, Yad. Fiz, **30** (1979) 1368.

[12] A.S. Deakin, V. Elias, D.G.C. McKeon and M.D. Scadron, Mod. Phys. Lett. **A9** (1994) 2381.

[13] D. Ebert, H. Reinhardt and M.K. Volkov, in A. Faessler (ed.): Prog. Part. Nucl. Phys. **33** (1994) 1.

[14] D. Ebert, T. Feldmann, M.K. Volkov, Preprint Humboldt-University, Berlin Hub-EP-95/29 (1995).

[15] D. Ebert, Yu.L. Kalinovsky, L. Münchow, M.K. Volkov, Int. J. Mod. Phys. **A8** (1993) 1295;
Yu.L. Kalinovsky, M.K. Volkov, Yad. Fiz. **57** (1994) 1099.

[16] M.A. Ivanov and T. Mizutani, Phys. Rev. **D45** (1992) 1580.

[17] A.E. Dorokhov, M.K. Volkov, J. Hüfner, S. Klevansky and P.Rehberg, Preprint University Heidelberg HD-TVP-95-12 (1995).

[18] V. Bernard and D. Vautherin, Phys. Rev. **D40** (1989) 1615.

Received by Publishing Department
on April 12, 1996.